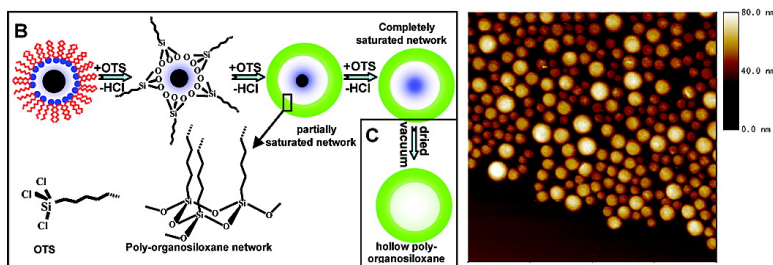


## Synthesis and Characterization of Monodisperse Poly(organosiloxane) Nanocapsules with or without Magnetic Cores

Anuj Shukla, Patrick Degen, and Heinz Rehage

*J. Am. Chem. Soc.*, **2007**, 129 (26), 8056-8057 • DOI: 10.1021/ja070502d • Publication Date (Web): 08 June 2007

Downloaded from <http://pubs.acs.org> on February 16, 2009



### More About This Article

Additional resources and features associated with this article are available within the HTML version:

- Supporting Information
- Access to high resolution figures
- Links to articles and content related to this article
- Copyright permission to reproduce figures and/or text from this article

[View the Full Text HTML](#)

## Synthesis and Characterization of Monodisperse Poly(organosiloxane) Nanocapsules with or without Magnetic Cores

Anuj Shukla, Patrick Degen, and Heinz Rehage\*

*Lehrstuhl für Physikalische Chemie II, Universität Dortmund, Otto-Hahn-Strasse 6, D-44227 Dortmund, Germany*

Received January 23, 2007; E-mail: heinz.rehage@uni-dortmund.de

Amphiphilic core-shell nanoparticles are of steadily growing interest.<sup>1–3</sup> Most work in this area has, however, been focused on the development of synthetic methodologies. Very little attention has been directed to the modification of the cores of these nanoparticles.<sup>4</sup> Here we describe the synthesis of poly(organosiloxane) nanocapsules which can be filled with suspensions of iron oxide nanoparticles (ferrofluids). The synthesis approach has two essential features: (1) the synthesis of iron oxide ( $\text{Fe}_3\text{O}_4$ ) nanoparticles induced by a chemical precipitation process in reverse micellar cavities (RMC);<sup>5</sup> (2) in situ preparation of the ultrathin poly(organosiloxane) shells around the aqueous ferrofluid droplet. The organic shell around the droplet surface was formed through the hydrolysis and poly condensation of octadecyl-trichlorosilane (OTS). During the polymerization process the original stabilizing surfactant shell was replaced by the very thin, coherent OTS-layer (Figure 1). The next major step in the nanocapsule formation was achieved by removing the magnetic iron nanoparticles by chemical etching processes. We finally obtained nanocapsules filled with an aqueous core. The possibility of encapsulating or entrapping different materials inside the nanospheres can be used to produce new types of microreactors.<sup>1–3</sup>

The physicochemical properties of the organic shell and the internal phase of the poly(organosiloxane) nanocapsules can be customized widely. Different network forming monomers offer a broad variability to tailor the wall design. The size of the nanocapsules can be controlled by varying the size of reverse micelles.

Figure 2 shows the DLS results and the schematic picture of the nanocapsules filled with ferrofluids (RMC@OTS). As shown in Figure 2, a change in the color of the RMC@OTS occurred a few minutes after the incorporation of OTS monomers. The final product was transparent and remained stable over months. Droplets containing  $\text{Fe}_3\text{O}_4$  nanoparticles were brown in color. With increasing concentration of OTS molecules the color of the samples changed to light brown (partial etching of  $\text{Fe}_3\text{O}_4$ ). For OTS concentrations above 12.8 mM the solutions became yellow (complete etching process: yellow color represents pure  $\text{FeCl}_3$  droplets). These observations provide evidence for chemical reactions, which occurred mainly inside the nanodroplets (formation of poly(organosiloxane) networks and the release of HCl during the polymerization: Figure S3 & S4).

The etching process of  $\text{Fe}_3\text{O}_4$  into  $\text{FeCl}_3$  was induced by the release of HCl into the aqueous phase. As shown in Figure 2A, an increase in OTS concentration led to the formation of smaller and more monodisperse nanocapsules.

The observed results can be explained by the formation of thin poly(organosiloxane) layers, which stabilized the droplet interfaces and reduced capsule interactions. This interpretation is consistent with our observation that the RMC@OTS nanocapsules show no secondary growth with time while the pure surfactant stabilized

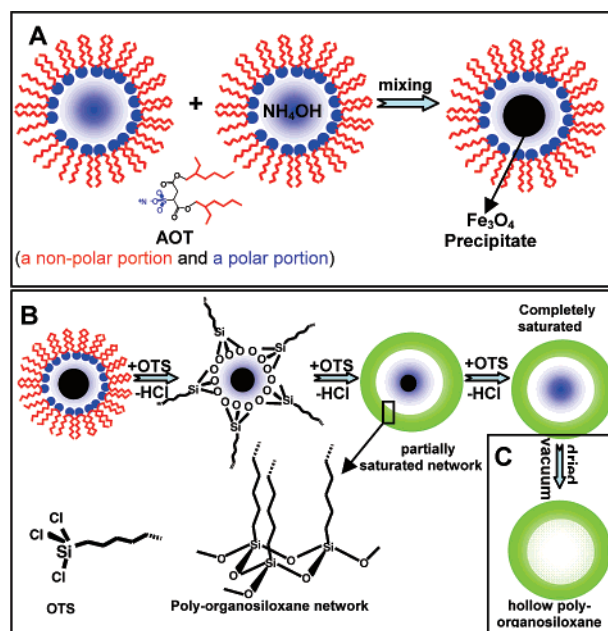


**Figure 1.** Schematic procedure used to generate hollow poly(organosiloxane) nanocapsules. (A) preparation of iron oxide nanoparticles in microemulsion; (B) polymerization of OTS around the water droplets and subsequent etching of the iron oxide nanoparticles; (C) monomer and surfactant were removed from the solution by four subsequent washing cycles with water. The nanocapsules were dried in vacuum, and we finally obtained redispersible nanocapsules.

$\text{Fe}_3\text{O}_4$  nanoparticles formed larger size particles with time (see Figure 2B–F).

Measurements of the plasmon-resonance-band (PRB) of the nanocapsules provided an indirect piece of evidence supporting the formation of RMC@OTS core-shell morphology. Figure 3 shows a typical set of UV-vis spectra comparing  $\text{Fe}_3\text{O}_4$  and RMC@OTS nanocapsules dispersed in isooctane solution. According to Figure 3,  $\text{Fe}_3\text{O}_4$  nanoparticles showed a broad PRB at 370–425 nm. This PRB corresponds well with that of  $\text{Fe}_3\text{O}_4$  nanoparticles.<sup>6</sup> With increasing concentration of OTS monomers the height of the PRB was decreasing (partial etching of  $\text{Fe}_3\text{O}_4$ ) and for concentrations above 12.8 mM, the height of PRB remained almost constant (complete etching). PRB showed a blue-shift for OTS concentrations less than 12.8 mM and a red-shift and narrow absorption peak at elevated OTS concentrations. The observed blue shift can be explained by the partial replacement of surfactant molecules by polymerizing OTS molecules at the oil/water interface. This stabilization reduces the intermixing of the aqueous phase including the  $\text{Fe}_3\text{O}_4$  precipitate and leads to the formation of more rigid spherical nanodroplets. The red-shift and narrow absorption peak corresponds to the polycondensation and the evolution of the poly(organosiloxane) networks (Figure S1). Any shell formation with

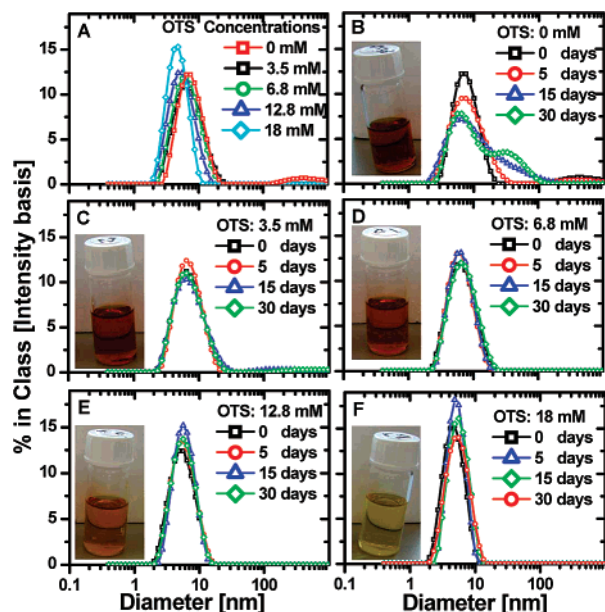


**Figure 2.** (A) Particle size distribution (PSD) of nanocapsules containing different amount of OTS monomers. (B–F) PSD of nanocapsules as a function of aging time containing different amount of OTS monomers: (B) 0 mM, (C) 3.5 mM, (D) 6.8 mM, (E) 12.8 mM, and (F) 18 mM.

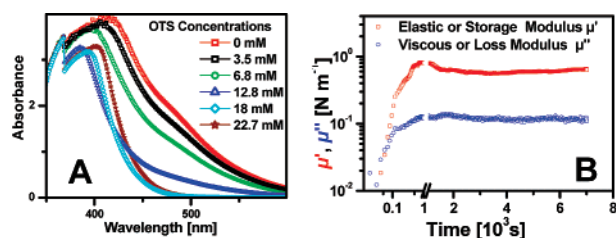


**Figure 3.** (A) UV-vis absorption spectra of nanocapsules containing different amounts of OTS monomers; (B) the two-dimensional storage ( $\mu'$ ) and loss ( $\mu''$ ) modulus of a polyorganosiloxane network as a function of reaction time.

a different refractive index from solvent will cause a shift in PRB. For OTS, with refractive index higher than iso-octane, we predict the observed red shift.<sup>7</sup>

To confirm that AOT surfactant molecules were replaced by OTS molecules, we performed a similar rheological experiment at the plane iso-octane/water interface. A 400 mM solution of AOT in water was poured into a beaker, and this AOT–water interface was covered with a 5 mM OTS solution in iso-octane. With a two-dimensional rheometer we measured the two-dimensional storage modulus ( $\mu'$ ) and loss modulus ( $\mu''$ ). As shown in Figure 3B, the increase of  $\mu'$  describes the evolution of the polysiloxane network as a function of reaction time. After a time span of approximately 5 min both moduli reach constant plateau values and the network formation is then complete. This fast reaction rate is consistent with the observed color changes of the  $\text{Fe}_3\text{O}_4$  solution within a few minutes after the addition of OTS. The dominant elastic modulus of the plateau regime confirms the formation of a cross-linked, two-dimensional polysiloxane network.

The RMC@OTS nanocapsules were purified by subsequent washing cycles with water to remove excess OTS monomers and surfactant molecules (Figure S2). The cleaned nanocapsules were

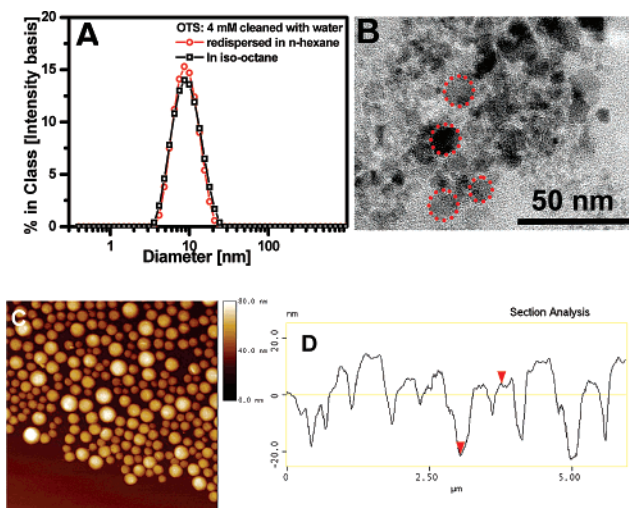


**Figure 4.** Particle size distribution (PSD) of original and purified nanocapsules: (A) DLS results; (B) TEM; (C, D) AFM images and section analysis. The scan size of the AFM image was  $10 \mu\text{m} \times 10 \mu\text{m}$ , and the size of the tip was 10 nm. OTS concentrations of 18 mM were used for TEM and AFM investigations.

dried in vacuum and redispersed in *n*-hexane for TEM and AFM analysis. The final suspensions remained transparent and stable over months. Figure 4A shows the size distribution of the original and redispersed nanocapsules. The results indicate that the purification method and liquid evaporation did not influence the particle size and shape. This suggests that this synthesis approach causes the formation of molecularly redispersible RMC@OTS nanocapsules. The TEM and AFM images of nanocapsules showed (Figure 4B,C) that the majority of the particles were spherical with typical diameters between 8 and 20 nm. The size of nanoparticles were estimated from the height of the particles using AFM. These values are in good agreement with the results of DLS experiments. These observations suggest that spherical shape was maintained after polymer coating, and the polymer shell did not collapse when liquid was evaporated. The poor quality of TEM images in comparison to AFM-images may be due to the low contrast of the polyorganosiloxane shells. The TEM images also showed some aggregation processes. This phenomenon was probably induced by attractive or magnetic interactions when the solvent was removed.

In summary, we have demonstrated a practical route to synthesize spherical, poly(organosiloxane) nanocapsules which can be filled with ferrofluids. This procedure can easily be modified to produce different types of magnetic responsible nanocapsules.

**Supporting Information Available:** Experimental details. This material is available free of charge via the Internet at <http://pubs.acs.org>.

## References

- (1) Lvov, Y.; Caruso, F. *Anal. Chem.* **2001**, *73*, 4212–4217.
- (2) Lvov, Y.; Antipov, A.; Mamedov, A.; Möhwald, H.; Sukhorukov, G. B. *Nano Lett.* **2001**, *1*, 125–128.
- (3) Tiourina, O. P.; Antipov, A. A.; Sukhorukov, G. B.; Larionova, N. L.; Lvov, Y.; Möhwald, H. *Macromol. Biosci.* **2001**, *1*, 209–214.
- (4) Kamata, K.; Lu, Y.; Xia, Y. *J. Am. Chem. Soc.* **2003**, *125*, 2384–2385.
- (5) Seip, C. T.; Carpenter, E. E.; O'Connor, C. *J. IEEE Trans. Magn.* **1998**, *34*, 1111.
- (6) Basu, S.; Chakravorty, D. *J. Non-Cryst. Solids* **2006**, *352*, 380–385.
- (7) Liz-Merzan, L. M.; Giersig, M.; Mulvaney, P. *Langmuir* **1996**, *12*, 4329–4335.

JA070502D